

Benchmark differential cross section ratios for excitation of the $5p^6\ ^1S_0 \rightarrow 5p^56s[3/2]_2$, $5p^56s[3/2]_1$, $5p^56s'[1/2]_0$ and $5p^56s'[1/2]_1 + 5p^56p[1/2]_1$ transitions in xenon at low incident electron energies.

A. Sakaamini, J-B. Faure, and M. A. Khakoo*
Department of Physics, California State University,
Fullerton, CA 92831, USA.

(Dated: March 10, 2021)

Benchmark intensity ratio measurements of the energy loss lines of xenon for excitation of the ground state $5p^6\ ^1S_0 \rightarrow 5p^56s[3/2]_2$, $5p^56s[3/2]_1$, $5p^56s'[1/2]_0$ and $5p^56s'[1/2]_1 + 5p^56p[1/2]_1$ transitions are reported, these being the lowest electronic excitations for xenon. The importance of these fundamental standards as a stringent test of theoretical electron scattering models is discussed for the rare gases as well as the role of spin-exchange and direct processes regarding the angular scattering behavior of these ratios.

PACS numbers: 34.80 Dp

The noble gases are useful species as buffers in plasmas and are of interest in spectroscopy and collision physics, because of their rich target structure involving spin-exchange and spin-orbit coupling relativistic effects both in the target structure and the scattering (continuum) electron [1]. Recent computational treatments of electron impact excitation and ionization processes involving multi-electron atomic target systems have made significant advances in electron collisions with light targets such as H [2], He [3] and H₂ [4] as well as light rare gas targets, Ne and Ar [5–8]. However, much improvement needs to be made regarding the heavier rare gases of Kr and Xe as was reported by Zatsarinny and Bartschat, regarding benchmark calculations on these very heavy targets [9]. Disagreements between the theory and experiment even for angle-integrated cross sections were labeled as being due to absolute normalization in the experiments [6]; a problem that has been difficult to overcome systematically e.g. when normalizing inelastic scattering features to the elastic scattering feature as a standard, this being due to the determination of instrumental detection efficiency for elastic and inelastic scattering. Recently we built an electron time-of-flight spectrometer to determine accurate elastic-to-inelastic differential electron scattering *ratios* for the excitation of the $X^1\Sigma_g^+ \rightarrow b^3\Sigma_u^+$ transition in H₂ [10]. These benchmark ratios were found to be in excellent agreement with the breakthrough Convergent Close-coupling of the Australia Curtin University group, and further resulted in significantly improved theoretical and experimental DCSs for both elastic and inelastic processes for H₂.

Since it is possible to measure relative *ratios* in scattering experiments we decided to *revisit* inelastic scattering ratios for the lowest transitions in Xe to provide experimental benchmark ratios for future collision models. Such ratio measurements were earlier made by us in at the NASA-Jet Propulsion Laboratory (JPL)[11]. Bartschat and Zatsarinny [5] commend such relative in-

elastic scattering ratios in the rare gases as representing ‘a very sensitive test to the quality of the theoretical model’; here they were referring to Ne where they found excellent agreement with our Ne experimental ratios [12] using their B-spline R-matrix calculations. For atoms with more than two electrons, the B-spline R-matrix electron scattering model is the best model currently available and has made excellent progress for the rare gases providing benchmark electron scattering calculations with this model [13].

The present work thus focuses on ratios only, in an aim to draw attention to ratios as benchmarks. The present California State University (CSUF) electron spectrometer has been well-tested and is referenced in [14]. Xe energy loss spectra were acquired at incident energies (E_0) values of 9.5 eV, 10 eV, 12.5 eV, 15 eV, 17.5 eV and 20 eV for scattering angles (θ) ranging from 10° to 120° with a typical energy resolution of around 35-50 meV for an incident current of about 13 nA to 20 nA. E_0 was calibrated using the He⁻ 2²S resonance at 19.366 eV at $\theta=90^\circ$ [15] to an obtain an E_0 with accuracy of within 50 meV during the entire run at that E_0 value. The CSUF spectrometer and the earlier JPL spectrometer differ distinctly in that the former has used real apertures in the analyzer as opposed to virtual apertures in the latter. Additionally, the CSUF spectrometer has an aperture gas target collimation system as compared to the JPL’s hypodermic needle gas collimator. In the typical energy loss spectra obtained, total counts exceeded 300 for the weakest $5p^56s'[1/2]_0$ excitation, i.e a maximal statistical error of $\pm 6\%$ for this weakest excitation. The spectra were fitted using a multi-Gaussian line profile (usually 2 Gaussians) to the spectrum after the energy loss axis was experimentally calibrated and employed Xe spectroscopic energy values of Moore [16] to locate the lines. A typical energy loss spectrum is shown in Fig. 1 in which we label features: (1) $5p^56s[3/2]_2$, (2) $5p^56s[3/2]_1$ (3) $5p^56s'[1/2]_0$ and (4+5) $5p^56s'[1/2]_1 + 5p^56p[1/2]_1$, since our spec-

trometer's best energy resolution ($\simeq 35$ meV) was unable to resolve the 4 and 5 excitation features separated by 10 meV, and caused us to record 4 and 5 as one composite feature. From these spectral features we define 4 ratios from the relative intensities, $I_n(E_0, \theta)$, of these features $n = 1$ to 5 as:

$$r(E_0, \theta) \equiv \frac{I_1(E_0, \theta)}{I_3(E_0, \theta)}, \quad (1)$$

$$r'(E_0, \theta) \equiv \frac{I_2(E_0, \theta)}{I_{4+5}(E_0, \theta)}, \quad (2)$$

$$r''(E_0, \theta) \equiv \frac{I_1(E_0, \theta)}{I_2(E_0, \theta)}, \quad (3)$$

$$r'''(E_0, \theta) \equiv \frac{I_3(E_0, \theta)}{I_{4+5}(E_0, \theta)}. \quad (4)$$

We note, using intermediate-coupling expansions from the Cowan code for Xe [11, 17, 18], that features 1 and 3 are triplet LS states and thus excited from the (pure singlet) ground $5p^6\ ^1S_0$ state by singlet-triplet processes mediated by spin-exchange via electron-exchange or electron spin-flip through spin-orbit coupling. On the other hand, the features 2, 4 and 5 are a mixture of singlet and triplet LS states and are excited not only by the direct scattering processes, but also by spin-exchange or spin-flip processes. Thus the ratios r'' and r''' qualitatively compare the relative strengths of spin-exchange to direct scattering process. Similarly the ratio r compares the relative strength of spin-exchange processes for the triplet excitations of features 1 and 3, whereas ratio r' compares the relative strength of (mostly) direct processes for the mixed excitations of features 1 and 3, and more so at and near small scattering angles, where long range forces are prevalent and favor direct scattering. The detection efficiency of the scattered electrons by the electron analyser for different scattered residual energies was made by measuring the energy loss spectrum of He at $E_0 = 29$ eV and $\theta = 90^\circ$, which comprised the ionization continuum and whose relative intensity is known to an error of better than 5% [19]. The detection efficiency correction factors at $E_0 = 9.5$ eV and 10 eV were 1.0625 and $1.059 \pm 7.5\%$ for the r'' ratio. At higher E_0 values, this correction for r'' was below $\simeq 4\%$. The correction for r' (which involves levels that are further separated than those of r'') at $E_0 = 12.5$ eV and above was $1.075 \pm 7.5\%$ and decreased at higher E_0 values.

r'' : We first focus on r'' since this ratio was taken at all E_0 visited here. It is compared to the earlier experimental r'' values at 10 eV, 15 eV and 20 eV [11] and to the available B-spline R-matrix [9] which are considered

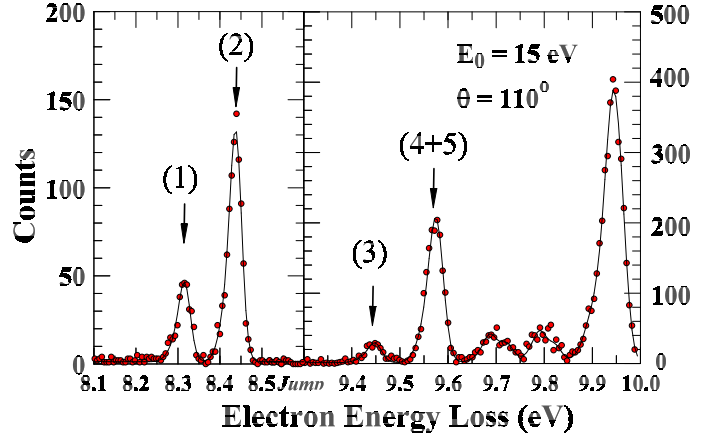


FIG. 1. Energy loss spectrum of Xe taken at E_0 of 15 eV and θ of 110° , defining the spectral features 1-5 in equations 1-4. The solid line is a linear least-squares fit to the spectrum used to unfold the spectrum to determine scattering intensities for the individual features.

benchmark calculations. Figure 2 shows our values of r'' . $E_0 = 9.5$ eV is only 0.053 eV above the threshold for exciting feature 3, viz. the $5p^56s'[1/2]_0$ level, so it was very weak. However, from the stronger features 1 and 2, at this E_0 the r'' ratio was experimentally determined. Our results show very good qualitative agreement with the B-spline R-matrix values of Zatsarinny and Bartschat [9, 20], but lie significantly below the theory at the maximum r'' at $\theta = 80^\circ$, by a factor of a factor about 30%. This maximum in r'' is clearly that of spin-exchange (over direct scattering). Our experiment in addition observes r'' increasing towards forward scattering θ of up to 20° . This forward scattering behavior is of interest since one would expect at these here the long range would disfavor spin-exchange, and r'' to fall toward small θ ; theory here also shows that spin-exchange process decreases with long range behavior. At E_0 of 10 eV, agreement between the earlier JPL and present CSUF experiments is excellent, well within error bars which typically are in the 8 to 10% range. However, the R-matrix does not show good agreement, displaying a maximum at $\theta < 85^\circ$, whereas the experiments show a shallow minimum at this angle, demonstrating how quickly dynamics can change from E_0 of 9.5 eV to 10 eV, near-threshold and confirming that the two experimental E_0 values are reliable. At $E_0 = 12.5$ eV some qualitative agreement is to be found between experiment and theory, but the r'' ratio decreases more at $\theta = 20^\circ$ than theory and still remains about 50% lower than theory at 80° . At $E_0 = 15$ eV agreement between experiments is excellent at $\theta \geq 30^\circ$. However, at 20° and 25° the present values are about 10-15% higher and r'' shows a maximum at 30° , but at large θ r'' keeps increasing showing rising spin-exchange. Theory is about 2 to 3 times higher at mid-angles around 90° . At $E_0 = 17.5$ eV the oscillatory angular behavior in r'' is absent

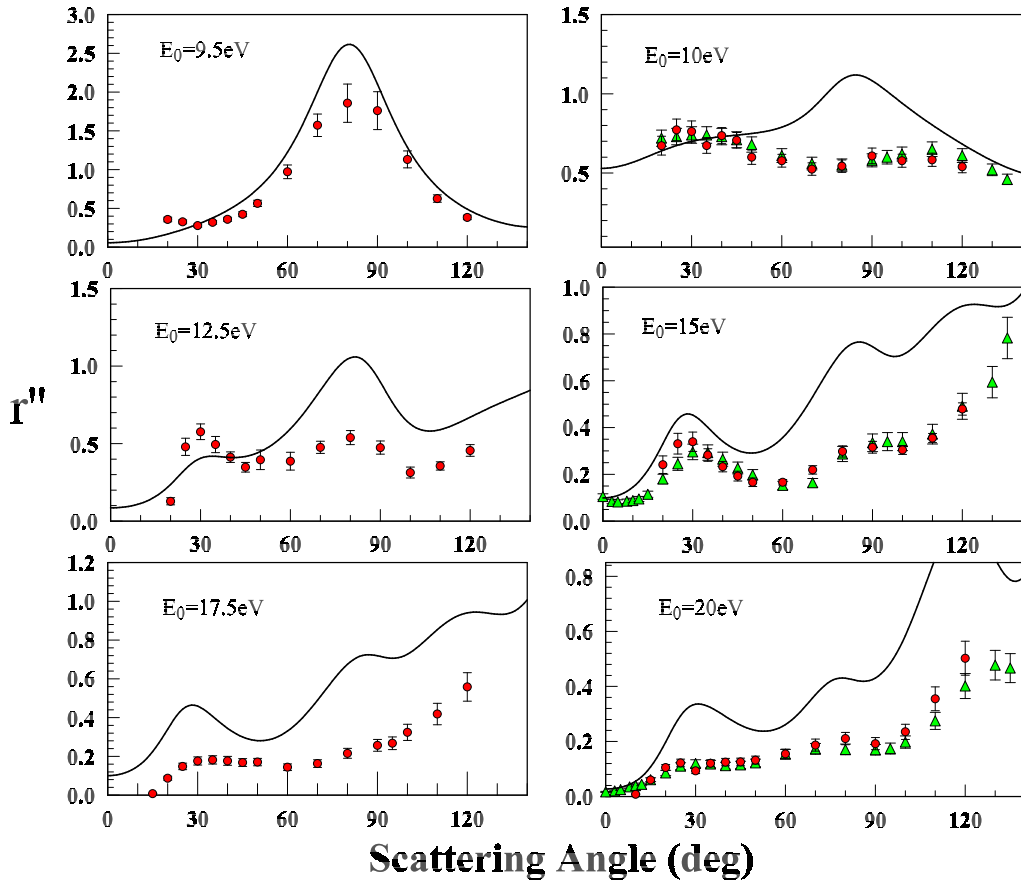


FIG. 2. r'' values for Xe. **Legend.** Experiments: red circles, present work; green triangles [11]. Theory: solid line, B-spline R-matrix model [9, 20].

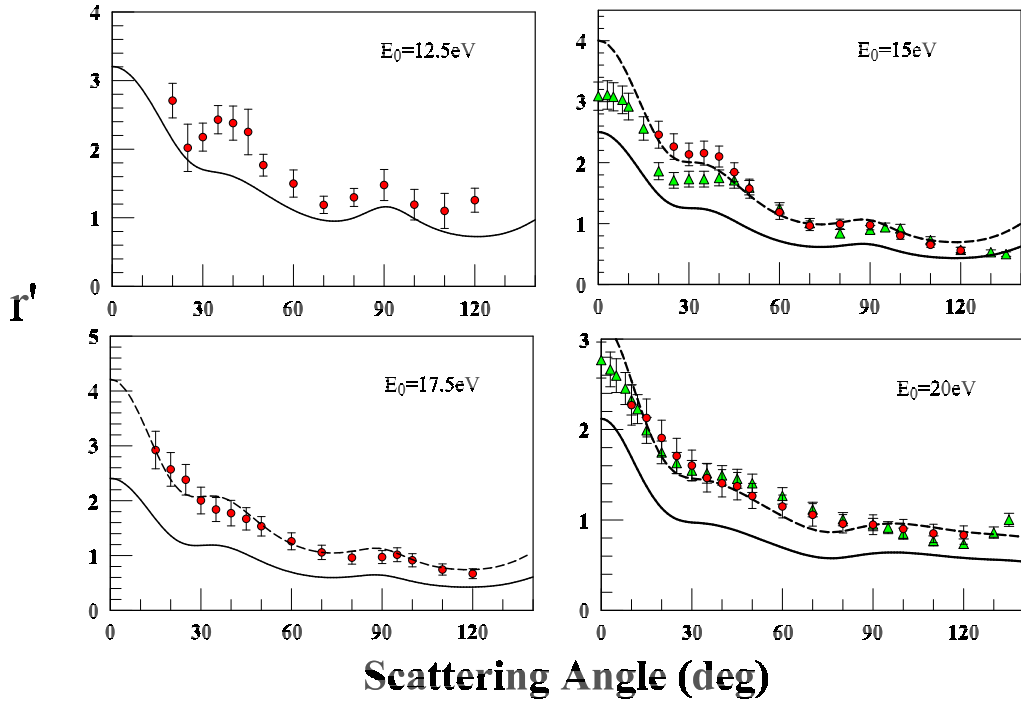


FIG. 3. r' values for Xe. Legend is the same as Figure 2, except dotted lines are scaled up values of r' of the solid lines. Scaling factors are given in the text.

in the experiment, but is prevalent in the theory which is quantitatively 3-4 times higher; this comparison continues into $E_0 = 20$ eV where agreement between the experiments is excellent throughout the angular range except at the smallest θ of 10° of the present experiment.

r': Figure 3 shows this ratio which compares the mixed singlet-triplet LS levels that exhibit long-range-forward scattering [11] via the direct (singlet) channel. We did not presently measure this ratio at $E_0 = 10$ eV, but instead at $E_0 = 12.5$ eV our experimental r' show good qualitative agreement with those of the R-matrix, except that the experimental r' is higher than theory by about 20% on average, outside of error bars. At $E_0 = 15$ eV the present results usefully correct our earlier values for θ of 20° to 35° by about 40%, producing improved quantitative agreement with the R-matrix, when it is multiplied by 1.6. At $E_0 = 17.5$ eV we again get excellent quantitative agreement with the R-matrix when it is multiplied by 1.75. At $E_0 = 20$ eV we see excellent agreement between the r' ratios of the experiments, and excellent quantitative agreement with theory when it is multiplied by 1.5. At small θ at 20 eV, theory rises noticeably faster than experiment. The fact that r' from R-matrix is qualitatively lower (by about 1.5) than experiment likely addresses the wave functions (mixing coefficients) used in the theory than in the dynamics, which would result in both qualitative and quantitative differences. The fact $J=1$ are strongly coupled states to the ground state and important for the theory to model better for in optical modeling (e.g. lifetime values, oscillator strengths). The other two ratios r and r'' will be discussed in a regular paper to follow this letter.

Interestingly our r'' at $E_0 = 9.5$ eV showing supposedly unusual increased small θ behavior of spin-exchange could also be related to a similar phenomenon observed by us in Ne regarding the electron impact orientation of the $2p^6\ ^1S_0 \rightarrow 2p^53s[1/2]_1\ ^1P_1$ excitation [7]. Here we observed, at E_0 of 25 eV, $\simeq 8$ eV above threshold, “unusual angular momentum transfer” in the scattering at θ around 25° , that caused a reversal of orientation of the 1P_1 perpendicular to the scattering plane. However, this state is not a pure 1P_1 LS state, being about 13% 3P_1 LS in character [12], and it could likely be that significant spin-exchange at small θ is pumping the reverse orientation, which is the only possible physical mechanism that can do this “reverse” pumping.

In the future, we intend to revisit such benchmark ratio measurements in Kr for the excitation of similarly placed $4p^6\ ^1S_0 \rightarrow 4p^55s$ transitions and similarly compare with our earlier CSUF measurements of Guo et al. [1] as well as the B-spline R-matrix model[20].

Briefly summarizing it is evident the the accurately reproducible nature of the ratios from (different) experiments is of use to provide benchmarks for testing future theoretical models and to shed light on physical processes

involved in the excitations.

This work was funded by the US National Science Foundation under Grant No. NSF-RUI AMO 1911702 which funded Dr. A. Sakaamini's Postdoctoral Fellowship. We also gratefully acknowledge the B-spline R-matrix results of [9] from Drs. Oleg Zatsarinny and Klaus Bartschat of Drake University, USA.

* mkhakoo@fullerton.edu

- [1] X. Guo, , S. Trajmar, V. Zeman, K. Bartschat, and C. J. Fontes, J. Phys. B: At. Mol. Opt. Phys. **32**, L155 (1999).
- [2] I. Bray and A. T. Stelbovics, Phys. Rev. A **46**, 6995 (1992).
- [3] I. Bray, D. V. Fursa, and I. E. McCarthy, J. Phys. B: At. Mol. Opt. Phys. **27**, L421 (1994).
- [4] M. C. Zammit, J. S. Savage, D. V. Fursa, and I. Bray, Phys. Rev. Letts. **116**, 233201 (2016).
- [5] O. Zatsarinny and K. Bartschat, Phys. Rev. A **86**, 022717 (2012).
- [6] O. Zatsarinny, Y. Wang, and K. Bartschat, Phys. Rev. A **89**, 022706 (2014).
- [7] L. R. Hargreaves, C. Campbell, M. A. Khakoo, O. Zatsarinny, and K. Bartschat, Phys. Rev. A **85**, 050701(R) (2012).
- [8] L. R. Hargreaves, C. Campbell, M. A. Khakoo, J. W. McConkey, O. Zatsarinny, K. Bartschat, A. D. Stauffer, and R. P. McEachran, Phys. Rev. A **87**, 022711 (2013).
- [9] O. Zatsarinny and K. Bartschat, J. Phys. B: At. Mol. Opt. Phys **43**, 074031 (2010).
- [10] M. Zawadzki, R. Wright, G. Dolmat, M. F. Martin, L. Hargreaves, D. V. Fursa, M. C. Zammit, L. H. Scarlett, J. K. Tapley, J. S. Savage, I. Bray, , and M. A. Khakoo, Phys. Rev. A **97**, 050702(R) (2018).
- [11] M. A. Khakoo, S. Trajmar, L. R. LeClair, I. Kanik, G. Csanak, and C. J. Fontes, J. Phys. B: At. Mol. Opt. Phys. **29**, 3455 (2008).
- [12] M. A. Khakoo, J. Wrkich, M. Larsen, G. Kleiban, I. Kanik, S. Trajmar, M. J. Brunger, P. J. O. Teubner, A. Crowe, C. J. Fontes, R. E. H. Clark, V. Zeman, K. Bartschat, D. H. Madison, R. Srivastava, and A. D. Stauffer, Phys. Rev. A **65**, 062711 (2002).
- [13] O. Zatsarinny and K. Bartschat, J. Phys. B: Conference Series **488**, 012044 (2014).
- [14] M. A. Khakoo, C. E. Beckmann, S. Trajmar, and G. Csanak, J. Phys. B: At. Mol. Opt. Phys. **27**, 3159 (1994).
- [15] J. H. Brunt, G. C. King, and F. H. Read, J. Phys. B: At. Mol. Opt. Phys. **10**, 1289 (1977).
- [16] C. E. Moore, *Atomic Energy Levels*, NSRDS-NBS Publication, Vol. 35 (US Govt Publishing, Washington. DC, 1957).
- [17] R. D. Cowan, *The Theory of Atomic Structure and Spectra* (University of California Academic Press, Riverside, California, 1981).
- [18] C. J. Fontes, Private Communication (1996).
- [19] E. Schow, K. Hazlett, J. G. Childers, C. Medina, G. Vitug, I. Bray, D. V. Fursa, and M. A. Khakoo, Phys. Rev. A **72**, 062717 (2005).
- [20] O. Zatsarinny and K. Bartschat, Private Communication (2021).